Hindawi
Advances in Civil Engineering
Volume 2019, Article ID 1360620, 11 pages
https://doi.org/10.1155/2019/1360620

Research Article

Behaviour of Rubberized Concrete Short Columns Confined by Aramid Fibre Reinforced Polymer Jackets Subjected to Compression

Gabriel Oprişan,[1] Ioana-Sorina Enţuc,[1] Petru Mihai,[2] Ionuţ-Ovidiu Toma,[3] Nicolae Ţăranu,[1] Mihai Budescu,[3] and Vlad Munteanu[1]

[1]*The "Gheorghe Asachi" Technical University of Iaşi, Faculty of Civil Engineering and Building Services, Department of Civil and Industrial Engineering, No. 1, Prof. dr. doc. D. Mangeron, 700050 Iaşi, Romania*
[2]*The "Gheorghe Asachi" Technical University of Iaşi, Faculty of Civil Engineering and Building Services, Department of Concrete Structures, Building Materials, Technology and Management, No. 1, Prof. dr. doc. D. Mangeron, 700050 Iaşi, Romania*
[3]*The "Gheorghe Asachi" Technical University of Iaşi, Faculty of Civil Engineering and Building Services, Department of Structural Mechanics, No. 1, Prof. dr. doc. D. Mangeron, 700050 Iaşi, Romania*

Correspondence should be addressed to Ionuţ-Ovidiu Toma; ionut.ovidiu.toma@tuiasi.ro

Received 26 September 2018; Revised 21 November 2018; Accepted 29 November 2018; Published 20 February 2019

Academic Editor: Carlos Chastre

The paper presents experimental and numerical investigations on the behaviour of rubberized concrete short columns confined with aramid fibre reinforced polymer (AFRP) subjected to compression. Additionally, the possibilities to substitute fine aggregate with crumb rubber granules, obtained from discarded worn tires, in structural concrete is also assessed. Because replacing traditional concrete aggregates by rubber particles leads to a significant loss in compressive strength, the authors highlight the use of AFRP confinement to partially or fully restore the compressive strength by applying a number of 1, 2, and 3 layers. Analytical models available for confined regular concrete are used to predict the peak stresses and the corresponding peak strains. Some analytical models give accurate results in terms of peak stress while others better approximate the ultimate strain. The full stress-strain curve of rubberized concrete and the experimentally obtained values for the material properties of AFRP are used as input data for the numerical modelling. A good agreement is found between the results obtained for the peak stress and corresponding axial strain from both the numerical simulations and the experimental investigations.

1. Introduction

The use of rubber aggregates, obtained from recycling end-of-life tires (ELT), in the construction industry amounts to an estimated 135,000 tonnes in Europe, meaning only 12% of the annual ELT output [1]. To date, rubberized concrete (RuC), that is traditional concrete in which a percentage of natural aggregates is replaced by rubber crumbs, has been used in construction industry for isolated foundations of the rotating machines to improve the damping of the vibrations, in platforms of the railway stations, support layers for buried pipes, road asphalt mixtures [2], paving systems and wearing layers for floors [3], acoustic and road side barriers [4], and the structural elements of shock dampers [5].

From the early research works [6], it was clear that substituting natural aggregates by rubber particles has led to a significant drop in the compressive strength. Subsequent investigations [7–9] confirmed earlier findings and highlighted the improved damping properties of rubberized concrete [10–12]. The optimization of the rubberized concrete mix, although a complex task, may lead to high-value applications from the point of view of sustainability [13].

It is commonly agreed on the fact that in order to utilize the rubberized concrete in structural applications, confinement

needs to be provided either internally [14], by means of fibres, or externally [15–17], by means of different types of fabrics embedded in polymeric resins. The use of rubberized concrete (RuC) in structural applications, as reported in the scientific literature, is quite limited [18–21]. Further studies are required before RuC becomes a material of choice for construction engineers.

Besides the clear benefits of using external confinement and especially with the new types of composite materials [22], a fresh set of problems had to be solved by the scientists, namely, the analytical models describing the behaviour of the newly resulted structural element [23, 24]. The first mathematical models of confined concrete by fibre-reinforced polymer (FRP) wraps had as a starting point the already existing equations developed for assessing the confining effect of traditional reinforcing cages in concrete elements [25–27].

With the increase in the number experimental tests on compressed FRP confined columns, bilinear forms of the models [28–30] or trilinear shapes have been developed [31, 32]. To this day, the study of the confining effect of FRP wraps on RC square columns made of OPC concrete is still an issue that needs more attention [33] first and foremost because of the complex behaviour due to the nonuniform lateral deformations along the perimeter of the cross section [34, 35]. The vast majority of research works focus on traditional concrete, without any inclusions of recycled materials, as it is the most widely used construction material. However, the proposed models available in the scientific literature address a wide range of compressive strength values as well as various types of FRP wraps [22, 32, 33, 36, 37].

2. Research Significance

The paper presents the results obtained in a research project the aim of which was the applicability of rubberized concrete in construction industry for load bearing elements. The short columns presented in this study are part of an RC model, shown in Figure 1, tested on various loading conditions, including lateral loads. Given the sharp decrease in the compressive strength of concrete when natural aggregates are replaced by rubber particles [9], the laboratory investigations aimed at confirming the suitability of using RuC in civil engineering structures.

The short columns were confined using AFRP jacket. The confinement was carried out to (a) restore the initial compressive strength of concrete [15] and (b) prevent the occurrence of the shear failure in the short columns [38] when the RC model was subjected to various loading scenarios [36].

Given the limited number of papers related to structural applications of RuC, the findings of the research work presented in here are certainly adding some of the needed information.

3. Materials and Methods

3.1. Materials. If the study was to have an impact from the point of view of recycling and saving natural resources, then one of the frequently and widely used types of concrete should be considered. A target compressive strength class C25/30 concrete was considered since it is one of the most widely used type of concrete for structural members in the construction industry.

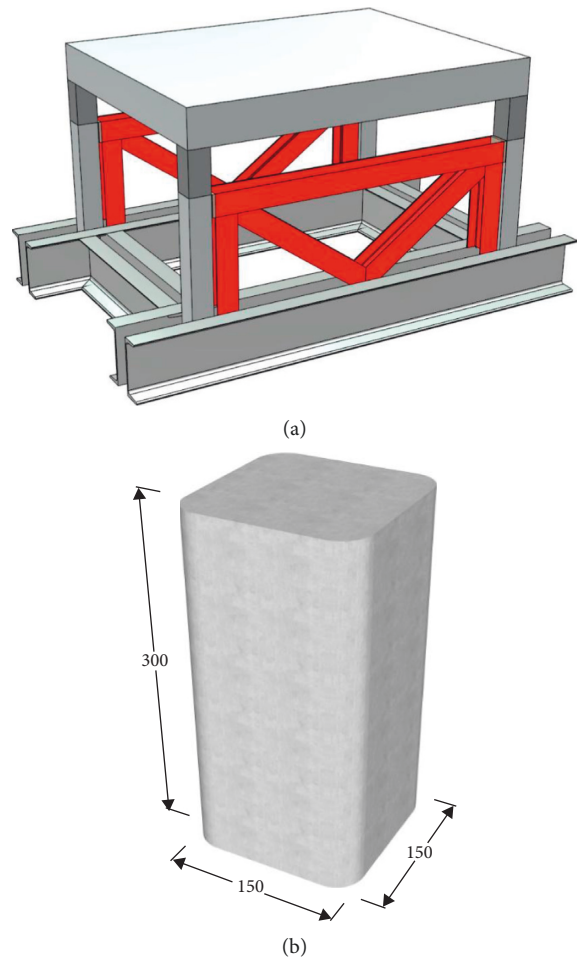

Figure 1: The scaled-down structural model and the short column.

The cement was a CEM I 42.5R type, readily available on the market. The natural aggregates were river aggregates without sharp edges to avoid the initiation and propagation of cracks due to stress concentrations.

The rubber crumbs came from a local supplier, and they were obtained from recycling discarded ELT. The rubber aggregates were examined for either textile or steel impurities before being used in the concrete mix. For the purpose of this research, two grain size intervals were taken into account: 0–4 mm to replace the sand and 4–8 mm to replace small coarse aggregates. The mix proportion for the rubberized concrete is shown in Table 1.

The replacement percentage of the natural aggregates by rubber particles was 40% by volume. The material characteristics of the aramid fibres and the bicomponent epoxy resin are given in Tables 2 and 3, respectively.

3.2. Methods. The rubber aggregates were weighted to assess their density [9]. The obtained values were similar to those reported by other researchers [12].

Table 1: The mixing proportion of concrete with the addition of rubber granules.

Mixing proportions (kg/m^3)						
W/C	Cement	Sand	Aggregate 4–8 mm	Aggregate 8–16 mm	Rubber* 0–4 mm	Rubber* 4–8 mm
0.47	489	488.59	294.59	646.7	93.41	93.41

*Table values correspond to 40% of the 0–4 mm fine aggregate and 4–8 mm small coarse aggregate.

Table 2: Characteristics of the aramid fibres.

Density (g/cm^3)	1.45
Elastic modulus (kN/m^2)	≥120
Tensile strength (N/mm^2)	≥2900
Elongation at rupture (%)	2.5
Design thickness (mm)	0.2

Table 3: Bicomponent epoxy resin characteristics.

Density (g/cm^3)	1.11
Glass transition temperature (°C)	44
Tensile strength after 14 days (N/mm^2)	35.8
Modulus of elasticity static after 14 days (N/mm^2)	2581.8
Modulus of elasticity dynamic after 14 days (N/mm^2)	2515 at +20°C 2989 at −20°C
Elongation at break (%)	2.3

The specimens were cast in vertical position, in wooden moulds, and were compacted with an electrical vibrator. Care was taken not to excessively vibrate the moulds to prevent the rising of the rubber particles at the top of the specimens. The rounding of the corners was obtained by placing in the casting mould four chamfered battens with a radius of 2.5 cm. This was done in order to ensure that the confinement with aramid FRP will work as intended and that there are no gaps between the fabric and the RuC column, especially at the corners [39]. Confinement effectiveness increases with an increase in corner radius and decreases with an increase in the sectional aspect ratio [22, 37, 40].

The fibres, the epoxy matrix, and the aramid FRP (AFRP) were subjected to uniaxial tensile tests, along the fibre direction, to assess their mechanical properties [41]. The obtained stress-strain curves are shown in Figure 2, and the average recorded values for the AFRP specimens correspond to a fibre volume fraction $V_f \approx 27\%$, a tensile strength of 506.8 MPa, and a corresponding tensile strain of 2.25%. The results were later used in the numerical modelling as input data.

The confinement procedure was hand wrapping of AFRP around the RuC short columns in 1, 2, and 3 layers using a brush to saturate the fibres with epoxy resin and a roller to remove the excessive resin and the entrapped air. The fibres orientation was in the hoop direction and a 100 mm overlap was considered in all cases in order to ensure a good anchorage and prevent debonding during the compression tests [39].

The main parameters of the research were the volume percentage of natural aggregate replacement by rubber particles and the number of AFRP confining layers. A total of

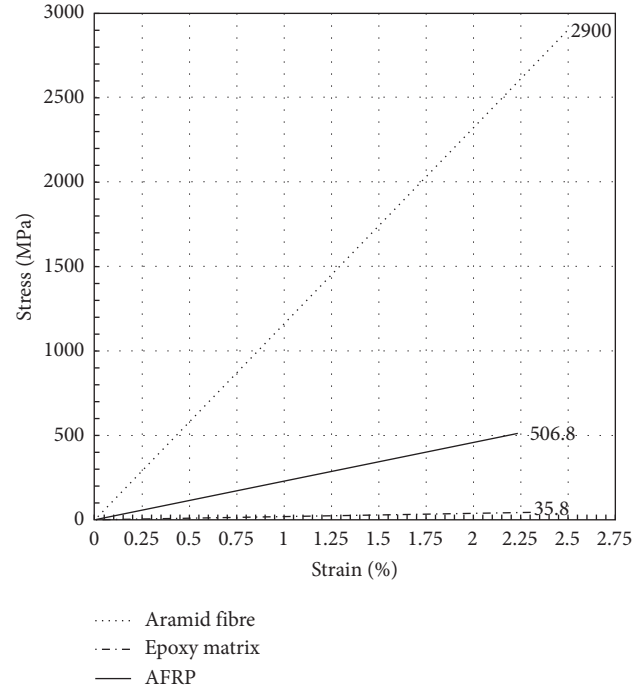

Figure 2: Tensile stress-strain curves of aramid fibre, epoxy matrix, and AFRP coupon with volume fraction $V_f \leq 27\%$.

20 short columns, 150 × 150 × 300 mm ($b \times h \times L$), were cast and tested at the age of 28 days. Five specimens were considered for the reference concrete mix and for each confining scenario (1, 2, and 3 layers of AFRP). Prior to testing, each short column was instrumented with strain gauges both in the hoop direction and along the loading direction, Figure 3(a). In addition, the specimens were also instrumented with linear-variable displacement transducers (LVDTs), Figure 3(b), that were used to obtain the complete stress-strain curve under compression by means of a patented device developed in the laboratory [42].

The uniaxial compression tests were carried out with the help of a 3000 kN universal testing machine at a constant loading rate of 0.2 MPa/s (4.5 kN/s). The data were recorded with the help of a data acquisition system capable of recording 100 kSamples/s/channel.

4. Results and Discussions

4.1. Stress-Strain Curve of Unconfined Rubberized Concrete Short Columns. Figure 4 shows the average complete stress-train curve [42, 43] obtained for the short columns made of unconfined rubberized concrete. Previous research works

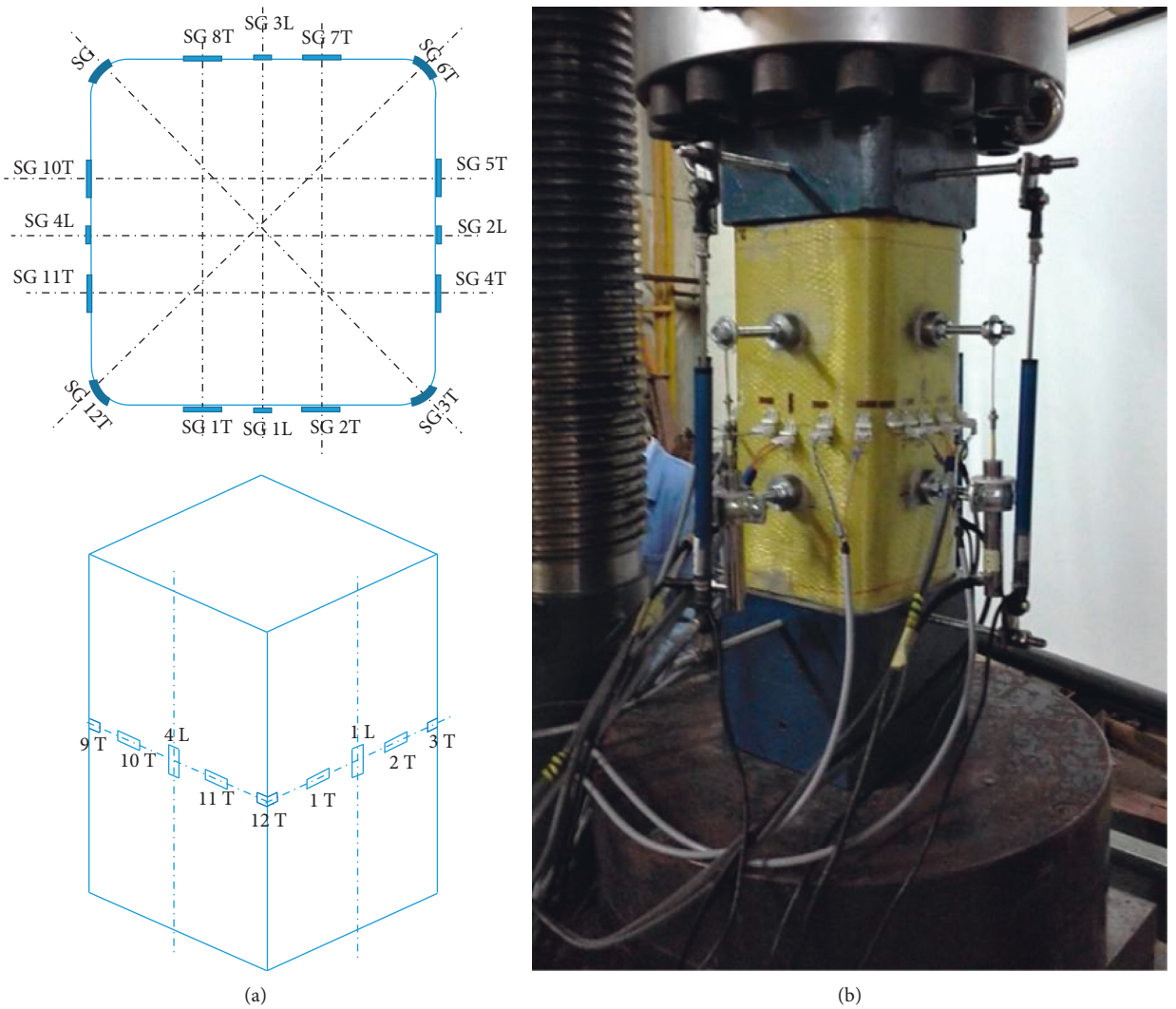

Figure 3: Arrangement of LVDT and strain gauges on the AFRP jacket. (a) Position of strain gauges. (b) Fully instrumented specimen.

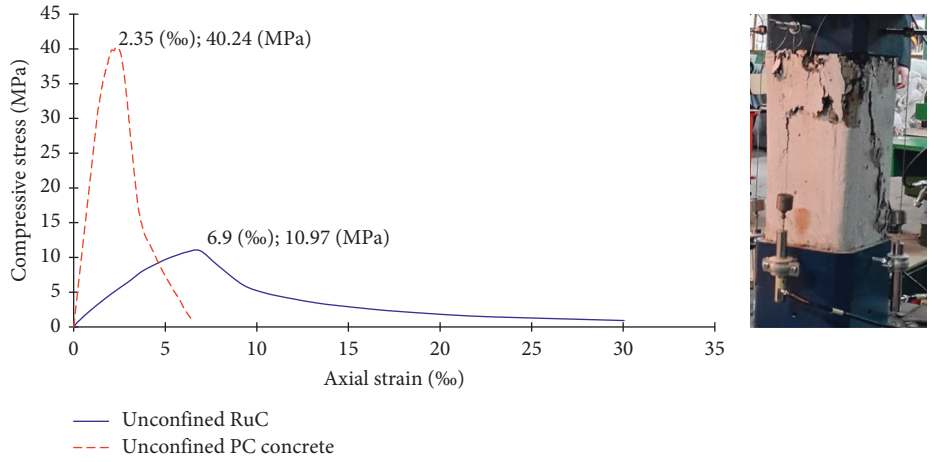

Figure 4: Complete stress-strain curve of normal and rubberized unconfined concrete columns and failure mode.

showed a significant decrease in the compressive strength compared to traditional concrete when natural aggregates were replaced by rubber particles [9, 43].

The average compressive strength from five samples of the short columns made of RuC was 10.97 MPa. The value is almost one-third of the target cylinder

compressive strength of 30 MPa needed for a C25/30 concrete class.

The complete stress-strain curve of the unconfined concrete was then used in the numerical model in order to assess the overall behaviour of the structure, Figure 1, subjected to different loading scenarios. The strain energy stored by the element in the postpeak region is almost similar in magnitude to the one stored in the prepeak region, including the linear-elastic range and the elasto-plastic range. This is a very important piece of information because it could explain the gradual decay of the structural characteristics of the model mainly due to the confining effect the steel reinforcing cage provides to the concrete core [27].

However, for RuC members in structural applications, additional confinement needs to be provided.

4.2. Stress-Strain Curve of AFRP Confined RuC Short Columns. External confinement was provided in the form of 1, 2, and 3 layers of AFRP. The overlap length was chosen 100 mm in order to prevent early debonding.

Figure 5 shows the average stress-strain curves for unconfined and the three cases of confined RuC short columns. Each curve was obtained as the average of five specimens for each confining scheme. One layer of AFRP with 100 mm overlapping has led to an increase of 191% in the compressive strength compared to the unconfined short column. Adding 2 and 3 layers of confinement has led to 295% and 363% improvement over the reference case, respectively. It can be observed that with two layers of AFRP, the concrete restored its target compressive strength of 30 MPa.

Additionally, confined RuC short columns exhibited larger axial strains corresponding to the peak stress compared with the unconfined specimens (6.9‰). The recorded values were 5.6 times larger for one layer of AFRP (39.4‰) and up to 10 times larger for three layers of confinement (70.02‰). It can be noticed that the ductility significantly improved in the case of confining with AFRP composite jackets. Table 4 summarizes the experimental results in terms of peak compressive stress and the corresponding strain.

Another benefit of using AFRP composite jackets was the increase in the upper limit of the linear-elastic range, Figure 6. The corresponding stress, also called in the scientific literature transitional compressive strength [44, 45], shows an increase proving the suitability of using AFRP wraps as strengthening solutions of RuC short columns.

However, the initial stiffness of the composite element did not show a significant change compared to the unconfined short column. This could be explained by the fact that during the linear-elastic range of the stress-strain curve, the behaviour is mainly governed by the rubberized concrete. With the increase in the axially applied load, the concrete swells, thus activating the AFRP jacket. Although a perfect bond is assumed between the concrete and the composite jacket from the very beginning, the experimental investigations show this is not entirely true. The benefit of using AFRP confinement is observed after the elastic limit is exceeded.

The value of failure strain of AFRP was also recorded by means of strain gauges, Figure 3(a), and it was less than the one obtained in pure tensile tests. This was due to the fact that besides tensile stresses, the AFRP jacket was also subjected to laterally applied pressure due to the dilatation of the rubberized concrete short columns.

4.3. Comparison with Analytical Solutions. The experimental results were compared with the classical analytical solutions [46, 47] frequently used by structural designers and proposed models found in the scientific literature for regular concrete elements [36, 37, 45, 48–51], Table 5. The parameters that influence the confinement effect produced by AFRP jacket are the volumetric ratio of AFRP jacket, the tensile strength of AFRP jacket, the tensile modulus of elasticity in the hoop direction, the ultimate tensile strength of AFRP, the compressive strength of unconfined rubberized concrete, and the rubberized concrete column dimensions including the corner radius [22, 40]. Generally, the formula for the strength model is based on a linear relationship between the confinement effectiveness factor f'_{cc}/f'_{c} and confinement ratio f'_{lc}/f'_{c} [45].

The normalized values, with respect to the experimentally obtained data, are presented in Figure 7, for the peak stress, and Figure 8, for the corresponding ultimate strain. $f'_{cc,theo}$ and $\varepsilon_{cc,theo}$ are the confined concrete strength and the ultimate strain of confined concrete computed by using the analytical models presented in Table 5.

Analysing the results shown in Figure 7, it can be observed that the ACI model [47], the Lam and Teng model [49], and Girgin model [50] give accurate results in terms of peak stress for one layer of confinement. For the specimens using two and three layers of AFRP, the *fib* [46] and Lam and Teng model [49] produce accurate results. The scattering of the results given by the analytical models becomes smaller with the increase in the number of layers. This could be explained by the fact that these models were developed for regular concrete, and with the increase in the number of confining AFRP layers, the RuC reaches the target compressive strength of concrete of 30 MPa.

The normalized ultimate strain values, Figure 8, present a larger scattering especially for the specimens confined with three layers of AFRP. For two of the three levels of confinement, the Girgin model [51] gives the best approximation of the experimental results. For the third case, the ACI model [47] yields slightly better results but not by a significant margin.

4.4. Numerical Analysis. The numerical analysis was conducted by means of ATENA Software, specially designed for the nonlinear analysis of concrete structures.

The numerical model of the short concrete column is shown in Figure 9. The concrete core was modelled via a CCIsoWedge solid element, Figure 10, [52]. In order to avoid any convergence errors, the layers of AFRP were modelled using the same element applied to the concrete core for which the thickness was changed to fit the thickness of the AFRP composite jacket. For the specimens having two or three layers

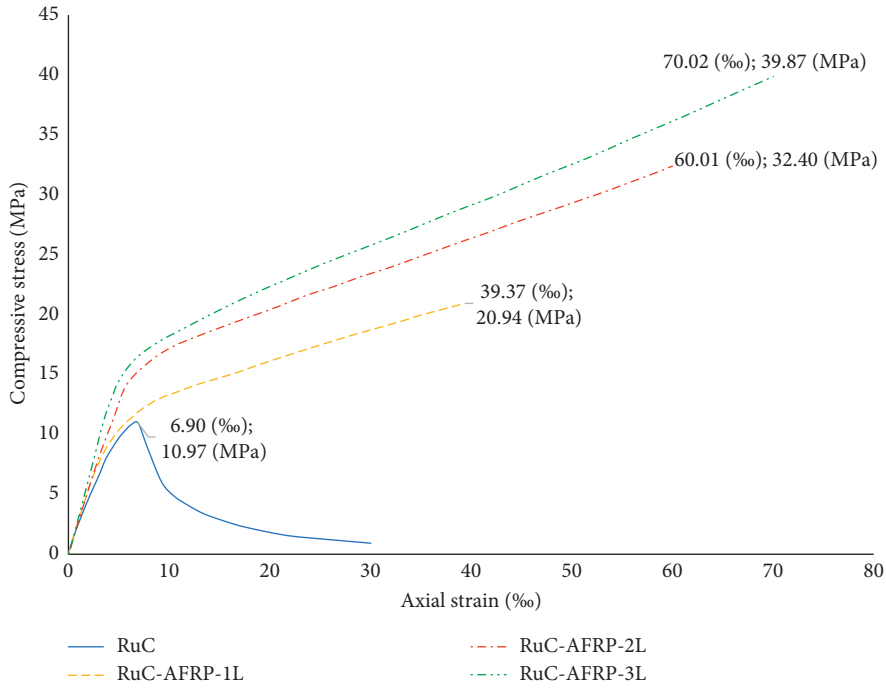

Figure 5: Average stress-strain curves of unconfined and AFRP-confined rubberized concrete short columns.

Table 4: Experimental values of confined rubberized concrete.

Specimen	Number of confining layers	f'_c (MPa)	f'_{cc} (MPa)	f'_{cc}/f'_c	ε_{cu} (‰)	ε_{ccu} (‰)	$\varepsilon_{ccu}/\varepsilon_{cu}$
RuC	0	10.97	—	—	6.9	—	—
RuC-AFRP-1L	1	—	20.94	1.91	—	39.37	5.71
RuC-AFRP-2L	2	—	32.40	2.95	—	60.01	8.70
RuC-AFRP-3L	3	—	39.87	3.63	—	70.02	10.15

f'_c: compressive strength of unconfined rubberized concrete short column (MPa). f'_{cc}: compressive strength of confined rubberized concrete short column (MPa). ε_{cu}: ultimate axial compressive strain of unconfined rubberized concrete short column (‰). ε_{ccu}: ultimate axial compressive strain of confined rubberized concrete short column (‰).

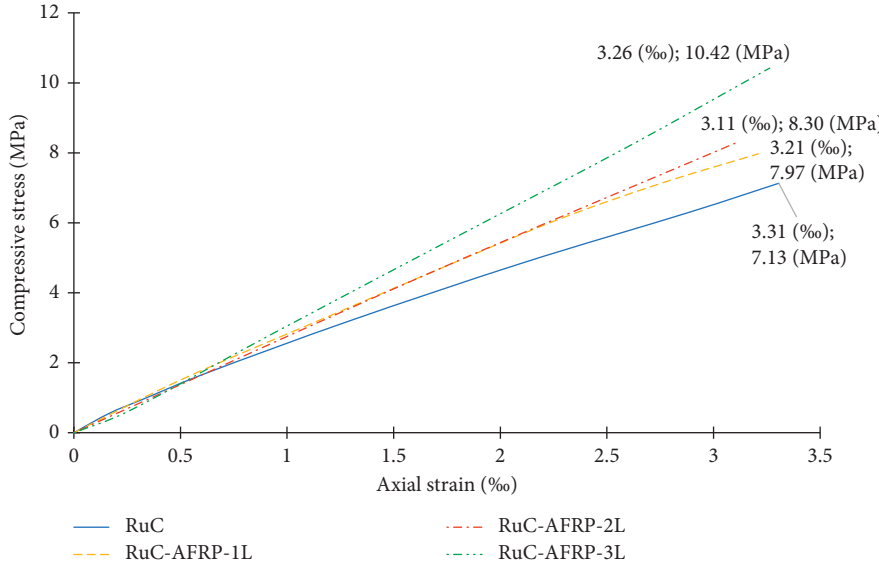

Figure 6: Elastic limit for the unconfined and AFRP confined rubberized concrete short columns.

Table 5: Confined concrete models for square concrete columns.

References standards and/or models	Compressive strength models	Ultimate axial strain	Confining pressure and coefficients
Fib, 2001 [46]	$f'_{cc}/f'_c = 2.254\sqrt{1+7.94(f_l/f'_c)} - 2(f_l/f'_c) - 1.254$	$\varepsilon_{cc}/\varepsilon'_c = 1 + 5(f'_{cc}/f'_c - 1)$	$f_l = \rho_f k_s E_f \varepsilon_{fu}$ $k_s = 1 - (2/3)((b-2r)/A_g(1-\rho_l))$
ACI committee 440, 2008 [47]	$f'_{cc}/f'_{cc} = (1 + 3.3(A_e/A_c)(f_l/f'_{co}))$	$\varepsilon_{cu}/\varepsilon_{co} = 1.5 + 12(A_e/A_c)(f_l/f'_{co})(\varepsilon_{frp}/\varepsilon_{co})^{0.45}$	$f_l = ((\sqrt{2}\,\varphi_f E_{frp}\varepsilon_{frp}t_{frp})/b)$ $\varphi_f = 0.95$, reduction factor
Shehata et al., 2001 [48]; (fco = 25–30 MPa), CFRP	$f'_{cc} = f'_{co}(1 + 0.85(f_l/f'_{co}))$	$\varepsilon_{cu} = \varepsilon_{co}[1 + 13.5(f_l/f'_{co})]$	$f_l = ((2f_{frp}t_{frp})/D)$
Youssef et al., 2007 [45]; (f_{co} = 25–35 MPa), CFRP, GFRP	$f'_{cc}/f'_{co} = 0.5 + 1.225(k_{e1}f_l/f'_{co})^{3/5}$	$\varepsilon_{cu} = [0.00433 + 0.26(k_{e1}f_l/f'_c)(f_{frp}/f'_c)^{1/2}]$	$f_l = ((2f_{frp}t_{frp}k_{e1})/D)$
Lam and Teng, 2002 [49]; (f_{co} = 27–55 Mpa)	$f'_{cc}/f'_{co} = (1 + 3.3(A_e/A_c)(f_l/f'_{co}))$	$\varepsilon_{cu}/\varepsilon_{co} = 1.75 + 12(f_l/f'_{co})(\varepsilon_{frp}/\varepsilon_{co})^{0.45}$	$f_l = ((2E_{frp}\varepsilon_{frp}t_{frp})/D)$
Girgin and Girgin, 2014 [50]; strength model (f_{co} = 7–24 MPa)	$f_{cc}/f_{co} = (1 + (M/B)(f_l/f'_{co}))^B$	$\varepsilon_{cu}/\varepsilon_{co} = -4.24(f_l/f_{co})^2 + 15.4(f_l/f_{co}) + 2.23$	$f_l = ((2E_{frp}\varepsilon_{frp}t_{frp})/D)$ $B = 1 - 0.0172(\log f_{co})^2$ $M = 0.0035f_{co}^2 - 0.0056f_{co} + 2.83$
Girgin, 2015 [51]; strain model, (f_{co} = 15–50 MPa), CFRP, GFRP			

f'_{cc}, f_{cc}: confined concrete strength; f'_{co}, f_{co}, f'_c: unconfined concrete strength; f_l: lateral confining pressure; A_e: cross sectional area of effectively concrete section; A_e: cross sectional area of concrete section; A_c: total area of concrete; A_g: gross area of column cross section with rounded corners; b: side lengths of square column cross section; $D = b\sqrt{2}$: the equivalent diameter, or the diagonal distance of the square cross section; r: radius of rounded corners; ρ_l: volumetric ratio of longitudinal reinforcement to gross cross section; k_{e1}: shape coefficient; ρ_k: the confinement stiffness ratio; ρ_ε: the strain ratio; E_{frp}: elastic modulus of FRP; ε_{frp}: axial strain of FRP; $\varepsilon_{co}, \varepsilon_c$: axial strain of unconfined concrete; ε_{cc}, ε_{cu}: ultimate strain of confined concrete.

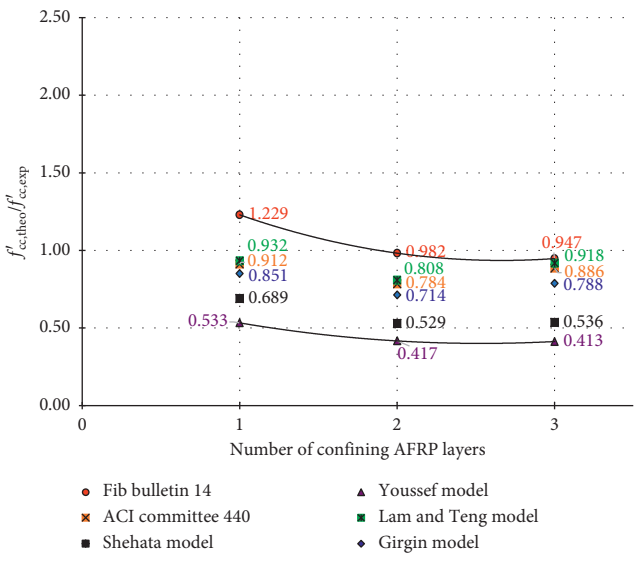

Figure 7: Normalized peak stress values.

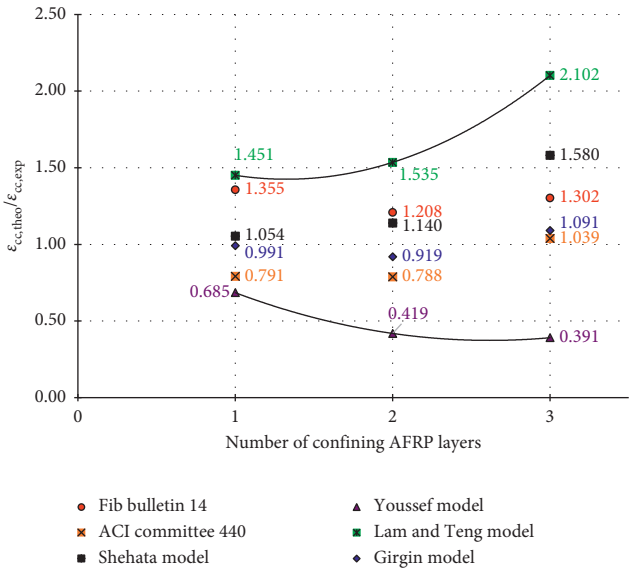

Figure 8: Normalized peak compressive strain.

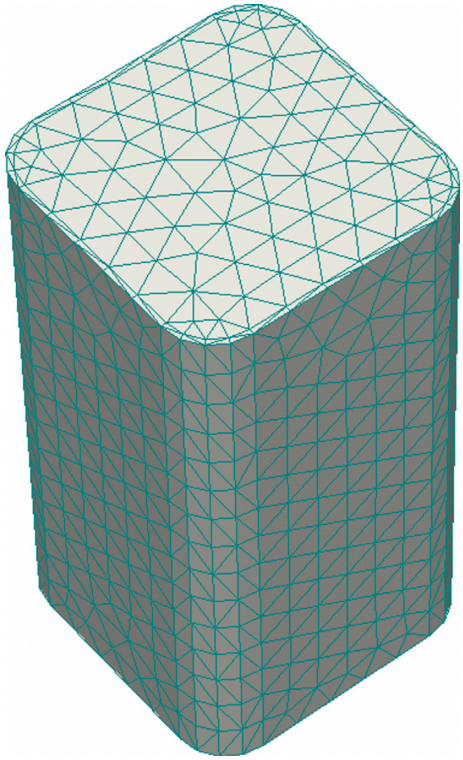

Figure 9: FEM model of the short RuC column.

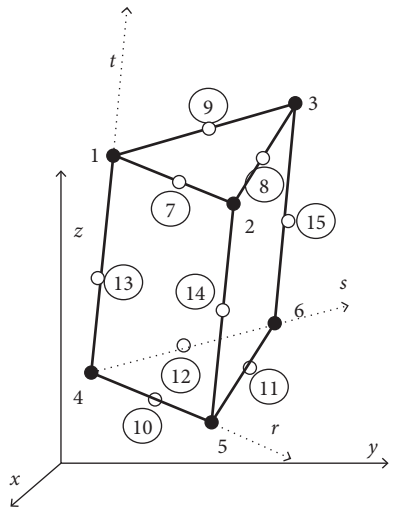

Figure 10: The CCIsoWedge solid elements used in the finite element model.

of confinement, the numerical model was generated with a single layer of AFRP having the appropriate thickness to match the specimens used during the laboratory investigations.

The material properties of RuC and AFRP jacket were experimentally determined and were used as input parameters in the numerical model. Stress-strain curve for each material has to be used as input data for nonlinear analysis in order to obtain accurate results, Figures 2 and 4. The material model used for the numerical analysis included a nonlinear behaviour of concrete in compression, fracture of concrete in tension, biaxial strength failure criterion, reduction of compressive strength after cracking, tension stiffening effect, and reduction of the shear stiffness after cracking [52].

The obtained results are presented in Figure 11. The stress-strain curves experimentally obtained are shown with solid lines while the results from the FE analysis are shown with dashed lines. It can be observed that there is a good agreement between the two types of stress-strain curves.

The stress-strain curves obtained by means of FEA show a higher initial stiffness compared to the experimental ones. This could be explained by the initial setting of the RuC short columns in the loading machine that could cause the instrumentation to record higher initial vertical deformations.

Additionally, a perfect bond assumption was considered in the numerical model which leads to the short columns having a higher stiffness. On the other hand, the perfect bond effect between the RuC and the AFRP jacket is becoming significant from higher compressive stress values, as shown in Figure 6.

The values of the peak compressive stress and the corresponding axial strain are summarized in Table 6. Both categories of results show very similar values.

5. Conclusions

The paper presents experimental and numerical investigations on the behaviour of rubberized concrete short columns confined with aramid fibre reinforced polymer subjected to compression. The aim is to check the suitability of using rubberized concrete for structural application. The AFRP wraps are used to restore the compressive strength of rubberized concrete that is significantly decreased when substituting the natural aggregates by rubber aggregates.

Based on the experimental and numerical investigations conducted during the research program, the following conclusions can be drawn:

(1) The complete stress-strain curves of unconfined normal and rubberized concrete were obtained. The strain energy stored in the postpeak region of the curve is similar in magnitude to the energy available in the prepeak region. In addition, the axial strain of the rubberized concrete corresponding to the peak stress is much larger than that in the case of regular concrete. This shows the improved deformability of the rubberized concrete columns.

(2) Confining the rubberized concrete columns with different number of AFRP layers leads to a full recovery of the concrete compressive strength lost by replacing the natural aggregates with rubber particles. In terms of axial behaviour of the short columns, the ultimate axial strain increases up to 10 times compared to unconfined specimens and depending on the number of AFRP layers used as confinement. The complete stress-strain curve of the confined rubberized concrete short columns cannot be determined due to the explosive failure of the jacket.

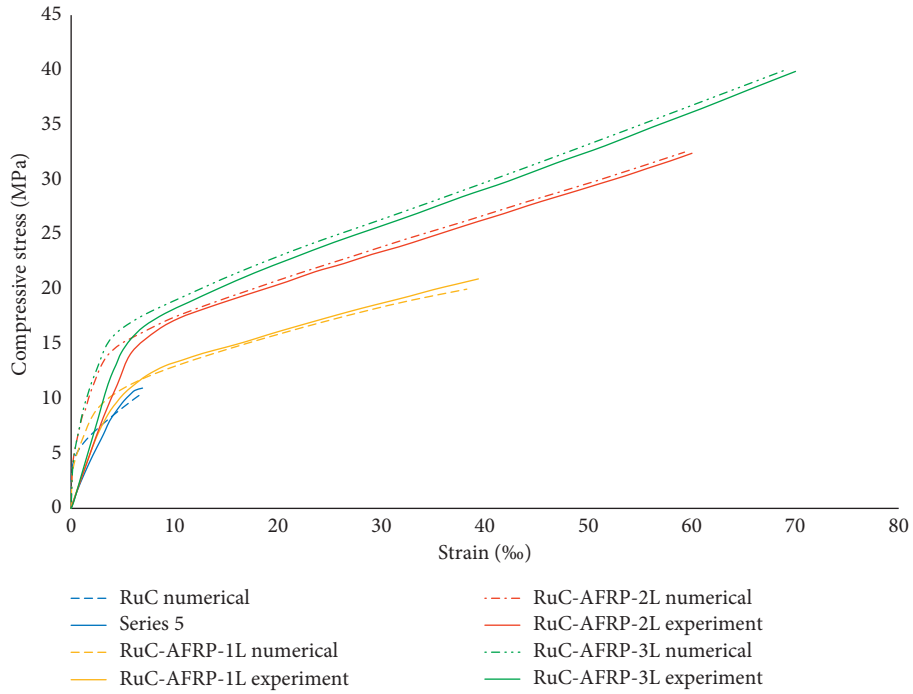

Figure 11: Numerical results vs experimental results.

Table 6: Experimental vs numerical simulations values.

Specimen	Number of confining layers	Experiment				Finite element analysis			
		f'_c (MPa)	f'_{cc} (MPa)	ε_{cu} (‰)	ε_{ccu} (‰)	f'_c (MPa)	f'_{cc} (MPa)	ε_{cu} (‰)	ε_{ccu} (‰)
RuC	0	10.97	—	6.9	—	10.5		6.86	—
RuC-AFRP-1L	1	—	20.94	—	39.37	—	20.00	—	38.25
RuC-AFRP-2L	2	—	32.40	—	60.01	—	32.50		59.29
RuC-AFRP-3L	3	—	39.87		70.02	—	40.00	—	69.05

(3) The analytical models that are currently applied to characterize the behaviour of confined regular concrete can be selectively applied to rubberized concrete. Some of the readily available models give accurate results while others are less suitable. However, there is a starting point and the analytical models applied to regular concrete could be changed to be more appropriate for rubberized concrete. This, however, can be achieved by further research in the field.

(4) The numerical investigations by means of FEM lead to accurate results in terms of peak stress and ultimate axial strain. The model fails to reproduce the initial behaviour of short rubberized concrete columns and overestimates the initial stiffness. This is caused by the perfect bond assumption between the rubberized concrete and the AFRP. Its effect is considered from the very beginning in the numerical model while during the experiments, it becomes evident from higher values of the compressive stress.

The results obtained at this stage of the research are encouraging from the point of view of the applicability of rubberized concrete in structural elements.

Data Availability

The data are under copyright provisions and will be made available on the FP7 project website https://ee.shef.ac.uk/projects/anagennisi-0.

Additional Points

Highlights. An experimental investigation of rubberized concrete short columns confined with AFRP confinement is presented. Replacement of 40% volume fraction of fine and small coarse aggregates by rubber particles from discarded tires diminishes the compressive strength. To compensate the decrease of compressive strength, the confinement with AFRP is utilized. Normalized axial compressive stress increases up to 363% in case of confinement with 3 layers of AFRP. The numerical simulation accurately predicts the peak stress and the corresponding axial strain of unconfined and confined rubberized concrete short columns.

Conflicts of Interest

The authors declare that there are no conflicts of interest regarding the publication of this paper.

Acknowledgments

This research was supported by FP7-ENV-2013-603722 "Innovative Reuse of All Tyre Components in Concrete ANAGENNISI" and Executive Unit for Financing Higher Education, Research, Development and Innovation (UEFISCDI) PNII-264EU/30.06.2014 from Romania.

References

[1] European Tyre and Rubber Manufacturers Association, "Annual report 2013/2014," 2014, http://www.srsa.gov.za/MediaLib/Home/DocumentLibrary/2013-14-SRSA-ANNUAL-REPORT.pdf.

[2] D. Lo Presti, "Recycled Tyre Rubber Modified Bitumens for road asphalt mixtures: a literature review," *Construction and Building Materials*, vol. 49, pp. 863–881, 2013.

[3] P. Sukontasukkul and C. Chaikaew, "Properties of concrete pedestrian block mixed with crumb rubber," *Construction and Building Materials*, vol. 20, no. 7, pp. 450–457, 2006.

[4] M. Elchalakani, "High strength rubberized concrete containing silica fume for the construction of sustainable road side barriers," *Structures*, vol. 1, pp. 20–38, 2015.

[5] R. Siddique, *Waste Materials and By-Products in Concrete*, Springer Berlin Heidelberg, Berlin, Heidelberg, 1st edition, 2008.

[6] N. I. Fattuhi and L. A. Clark, "Cement-based materials containing shredded scrap truck tyre rubber," *Construction and Building Materials*, vol. 10, no. 4, pp. 229–236, 1996.

[7] M. A. Aiello and F. Leuzzi, "Waste tyre rubberized concrete: properties at fresh and hardened state," *Waste Management*, vol. 30, no. 8-9, pp. 1696–1704, 2010.

[8] A. Fiore, G. C. Marano, C. Marti, and M. Molfetta, "On the fresh/hardened properties of cement composites incorporating rubber particles from recycled tires," *Advances in Civil Engineering*, vol. 2014, Article ID 876158, 12 pages, 2014.

[9] I.-O. Toma, N. Ţăranu, O.-M. Banu, M. Budescu, P. Mihai, and R.-G. Ţăran, "The effect of the aggregate replacement by waste tyre rubber crumbs on the mechanical properties of concrete," *Romanian Journal of Materials*, vol. 45, pp. 394–401, 2015.

[10] J. Xue and M. Shinozuka, "Rubberized concrete: a green structural material with enhanced energy-dissipation capability," *Construction and Building Materials*, vol. 42, pp. 196–204, 2013.

[11] L. Zheng, X. Sharon Huo, and Y. Yuan, "Experimental investigation on dynamic properties of rubberized concrete," *Construction and Building Materials*, vol. 22, no. 5, pp. 939–947, 2008.

[12] A. O. Atahan and A. Ö. Yücel, "Crumb rubber in concrete: static and dynamic evaluation," *Construction and Building Materials*, vol. 36, pp. 617–622, 2012.

[13] S. Raffoul, R. Garcia, K. Pilakoutas, M. Guadagnini, and N. F. Medina, "Optimisation of rubberised concrete with high rubber content: an experimental investigation," *Construction and Building Materials*, vol. 124, pp. 391–404, 2016.

[14] M. R. Hall and K. B. Najim, "Structural behaviour and durability of steel-reinforced structural Plain/Self-Compacting Rubberised Concrete (PRC/SCRC)," *Construction and Building Materials*, vol. 73, pp. 490–497, 2014.

[15] S. Raffoul, R. Garcia, D. Escolano-Margarit, M. Guadagnini, I. Hajirasouliha, and K. Pilakoutas, "Behaviour of unconfined and FRP-confined rubberised concrete in axial compression," *Construction and Building Materials*, vol. 147, pp. 388–397, 2017.

[16] O. Youssf, M. A. ElGawady, J. E. Mills, and X. Ma, "An experimental investigation of crumb rubber concrete confined by fibre reinforced polymer tubes," *Construction and Building Materials*, vol. 53, pp. 522–532, 2014.

[17] O. Youssf, M. A. ElGawady, and J. E. Mills, "Static cyclic behaviour of FRP-confined crumb rubber concrete columns," *Engineering Structures*, vol. 113, pp. 371–387, 2016.

[18] K. S. Son, I. Hajirasouliha, and K. Pilakoutas, "Strength and deformability of waste tyre rubber-filled reinforced concrete columns," *Construction and Building Materials*, vol. 25, no. 1, pp. 218–226, 2011.

[19] A. T. Noaman, B. H. A. Bakar, and H. M. Akil, "The effect of combination between crumb rubber and steel fiber on impact energy of concrete beams," *Procedia Engineering*, vol. 125, pp. 825–831, 2015.

[20] O. Youssf, M. A. ElGawady, and J. E. Mills, "Experimental investigation of crumb rubber concrete columns under seismic loading," *Structures*, vol. 3, pp. 13–27, 2015.

[21] P. Asutkar, S. B. Shinde, and R. Patel, "Study on the behaviour of rubber aggregates concrete beams using analytical approach," *Engineering Science and Technology, an International Journal*, vol. 20, no. 1, pp. 151–159, 2017.

[22] T. Ozbakkaloglu and E. Akin, "Behavior of FRP-confined normal- and high-strength concrete under cyclic axial compression," *Journal of Composites for Construction*, vol. 16, no. 4, pp. 451–463, 2012.

[23] Y. C. Wang and J. I. Restrepo, "Investigation of concentrically loaded reinforced concrete columns confined with glass fiber-reinforced polymer jackets," *ACI Structural Journal*, vol. 98, no. 3, 2001.

[24] G. Campione and N. Miraglia, "Strength and strain capacities of concrete compression members reinforced with FRP," *Cement and Concrete Composites*, vol. 25, no. 1, pp. 31–41, 2003.

[25] F. E. Richart, A. Brandtzæg, and R. L. Brown, *Failure of Plain and Spirally Reinforced Concrete in Compression*, University of Illinois, Champaign, IL, USA, 1929, http://hdl.handle.net/2142/4073.

[26] S. H. Ahmad and S. P. Shah, "Stress-strain curves of concrete confined by spiral reinforcement," *Journal of the American Concrete Institute*, vol. 79, no. 6, pp. 484–490, 1982.

[27] J. B. Mander, M. J. N. Priestley, and R. Park, "Theoretical stress-strain model for confined concrete," *Journal of Structural Engineering*, vol. 114, no. 8, pp. 1804–1826, 1988.

[28] A. Nanni and N. M. Bradford, "FRP jacketed concrete under uniaxial compression," *Construction and Building Materials*, vol. 9, no. 2, pp. 115–124, 1995.

[29] M. Samaan, A. Mirmiran, and M. Shahawy, "Model of concrete confined by fiber composites," *Journal of Structural Engineering*, vol. 124, no. 9, pp. 1025–1031, 1998.

[30] M. R. Spoelstra and G. Monti, "FRP-confined concrete model," *Journal of Composites for Construction*, vol. 3, no. 3, pp. 143–150, 1999.

[31] Y. Xiao and H. Wu, "Compressive behavior of concrete confined by carbon fiber composite jackets," *Journal of Materials in Civil Engineering*, vol. 12, no. 2, pp. 139–146, 2000.

[32] O. Chaallal, M. Hassan, and M. Shahawy, "Confinement model for axially loaded short rectangular columns strengthened with fiber-reinforced polymer wrapping," *ACI Structural Journal*, vol. 100, no. 2, pp. 215–221, 2003.

[33] P. Faustino and C. Chastre, "Analysis of load-strain models for RC square columns confined with CFRP," *Composites Part B: Engineering*, vol. 74, pp. 23–41, 2015.

[34] L. Chung-Sheng, *Modeling of FRP-jacketed RC Columns Subject to Combined Axial and Lateral Loads*, University of California, San Diego, CA, USA, 2006, https://escholarship.org/uc/item/02b530h8.

[35] G. Wu, Z. S. Wu, and Z. T. Lü, "Design-oriented stress-strain model for concrete prisms confined with FRP composites," *Construction and Building Materials*, vol. 21, no. 5, pp. 1107–1121, 2007.

[36] R. Eid and P. Paultre, "Compressive behavior of FRP-confined reinforced concrete columns," *Engineering Structures*, vol. 132, pp. 518–530, 2017.

[37] P. Faustino, C. Chastre, and R. Paula, "Design model for square RC columns under compression confined with CFRP," *Composites Part B: Engineering*, vol. 57, pp. 187–198, 2014.

[38] G. Promis and E. Ferrier, "Performance indices to assess the efficiency of external FRP retrofitting of reinforced concrete short columns for seismic strengthening," *Construction and Building Materials*, vol. 26, no. 1, pp. 32–40, 2012.

[39] G. Oprisan, N. Taranu, V. Munteanu, M. Budescu, C. Cozmanciuc, and R. Oltean, "Improvement of concrete strength through confining with composite materials," *Romanian Journal of Materials,*vol. 41, no. 4, pp. 302–315, 2011, http://solacolu.chim.upb.ro/pag_302_315web.pdf.

[40] L.-M. Wang and Y.-F. Wu, "Effect of corner radius on the performance of CFRP-confined square concrete columns: Test," *Engineering Structures*, vol. 30, no. 2, pp. 493–505, 2008.

[41] ASTM International, "ASTM D3039/D3039M-14 standard test method for tensile properties of polymer matrix composite materials," in *Annual Book of ASTM Standard*, pp. 1–13, 2014.

[42] A. Negoita, M. Budescu, R. Ciornei, L. Strat, N. Taranu, and I. Filipescu, "Metodă şi instalaţie pentru încercarea postelastică a materialelor, îndeosebi, a celor casante/method and instalation for postelastic behaviour assessment of brittle materials," Patent no. 77051, 1980.

[43] M. Budescu, P. Mihai, N. Ţăranu, I. Lungu, O.-M. Banu, and I.-O. Toma, "Establishing the complete characteristic curve of concrete loaded in compression," *Romanian Journal of Materials*, vol. 45, pp. 43–54, 2015.

[44] P. Rochette and P. Labossière, "Axial testing of rectangular column models confined with composites," *Journal of Composites for Construction*, vol. 4, no. 3, pp. 129–136, 2000.

[45] M. N. Youssef, M. Q. Feng, and A. S. Mosallam, "Stress-strain model for concrete confined by FRP composites," *Composites Part B: Engineering*, vol. 38, no. 5-6, pp. 614–628, 2007.

[46] International Federation for Structural Concrete (fib), *Externally bonded FRP reinforcement for RC structures*, International Federation for Structural Concrete, Lausanne, Switzerland, 2001, http://www.fib-international.org/externally-bonded-frp-reinforcement-for-rc-structures.

[47] ACI Committee 440, *Guide for the Design and Construction of Externally Bonded FRP Systems for Strengthening Concrete Structures-ACI 440.2R-08*, American Concrete Institute (ACI), Farmington Hills, MI, USA, 2008, https://www.concrete.org/store/productdetail.aspx?ItemID=440208.

[48] I. A. E. M. Shehata, L. A. V. Carneiro, and C. D. Shehata, "Strength of short concrete columns confined with CFRP sheets," *Materials and Structures*, vol. 35, no. 245, pp. 50–58, 2001.

[49] L. Lam and J. G. Teng, "Strength models for fiber-reinforced plastic-confined concrete," *Journal of Structural Engineering*, vol. 128, no. 5, pp. 612–623, 2002.

[50] Z. Girgin and K. Girgin, "A design-oriented combined model (7 MPa to 190 MPa) for FRP-confined circular short columns," *Polymers (Basel)*, vol. 7, no. 10, pp. 1905–1917, 2015.

[51] Z. C. Girgin, "Modified Johnston failure criterion from rock mechanics to predict the ultimate strength of fiber reinforced polymer (FRP) confined columns," *Polymers*, vol. 6, no. 1, pp. 59–75, 2014.

[52] V. Červenka, J. Jendele, and J. Cervenka, *ATENA Program Documentation. Part 1 Theory*, 2018, https://www.cervenka.cz/assets/files/atena-pdf/ATENA_Theory.pdf.